Biophysical Chemistry 149 (2010) 40–46

Contents lists available at ScienceDirect

Biophysical Chemistry

journal homepage: http://www.elsevier.com/locate/biophyschem

A thermodynamic analysis of fibrillar polymorphism

Martin D. Jeppesen [a,b,c], Kim Hein [c], Poul Nissen [c], Peter Westh [d], Daniel E. Otzen [a,b,c,*]

[a] Center for Insoluble Protein Structures (inSPIN), Interdisciplinary Nanoscience Centre, University of Aarhus, Gustav Wieds Vej 10C, DK-8000 Aarhus C, Denmark
[b] Department of Life Sciences, Aalborg University, Sohngaardsholmsvej 49, DK-9000 Aalborg, Denmark
[c] Department of Molecular Biology, University of Aarhus, Gustav Wieds Vej 10C, DK-8000 Aarhus C, Denmark
[d] Department NSM, Research Unit for Functional Biomaterials, Roskilde University, 1 Universitetsvej, DK-4000 Roskilde, Denmark

ARTICLE INFO

Article history:
Received 30 January 2010
Received in revised form 9 March 2010
Accepted 9 March 2010
Available online 9 April 2010

Keywords:
Glucagon
Fibrillation
Isothermal titration calorimetry
Fiber diffraction
Circular dichroism

ABSTRACT

We explore the thermodynamic properties of three different fibrils of the peptide hormone glucagon, formed under different salt conditions (glycine, sulfate and NaCl, respectively), and differing considerably in compactness. The three fibrils display a large variation in the specific heat capacity ΔC_p determined by isothermal titration calorimetry. Sulfate fibrils show a negative ΔC_p expected from a folding reaction, while the ΔC_p for glycine fibrils is essentially zero. NaCl fibrils, which are less stable than the other fibrils, have a large and positive ΔC_p. The predicted change in solvent accessible area is not a useful predictor of fibrillar ΔC_p unlike the case for globular proteins. We speculate that strong backbone interactions may lead to the unfavorable burial of polar side residues, water and/or charged groups which all can have major influence on the change in ΔC_p. These results highlight differences in the driving forces of native folding and fibril formation.

1. Introduction

The accumulation of insoluble protein deposits as fibrils or amyloid is associated with a growing number of neurodegenerative diseases such as Parkinson's and Alzheimer's, as well as systemic diseases like Senile Systemic Amyloidosis [1]. These fibrils consist of cross β-sheet structure where the β-strands are organized perpendicular to the long fibril axis. Although individual side chains can affect the fibrillation kinetics and the fibrillar architecture [2], it has been suggested that the ability to fibrillate is an intrinsic property of the polypeptide chain. Thus essentially all proteins can form these structures under appropriate conditions [3–5], with the obvious corollary that environmental factors have a substantial impact on protein folding, misfolding and aggregation. The end state can be dictated by kinetic accessibility as much as thermodynamic stability. This is illustrated in the concept of the energy landscape [6,7], where many environmental factors will influence the landscape's overall shape and ruggedness. One critical factor in this context is the interaction with the fluctuating "cloud" of water molecules solvating the protein surface [8], which is quantified through the solvent accessible surface area (ASA). Folding reduces ASA due to the increased compaction of the protein. Analyses of protein unfolding data and the thermodynamics of dissolution of aqueous model compounds have shown that ΔC_p may be expressed as a linear combination of the changes in polar (ΔASA_{pol}) and non-polar ($\Delta ASA_{non\text{-}pol}$) accessible surface area [9–11]. The coefficients that quantify the contributions from each type of surface area vary quite significantly in these studies, but they are always positive for non-polar and negative for polar surface, and the former is (numerically) 2–3 times larger than the latter. One important implication of this is that the characteristic increase in heat capacity following thermal unfolding relies on increased non-polar accessible surface area. The differences between polar and non-polar surface area may be averaged out so that ΔC_p can be estimated simply from the number of residues (n_{aa}) in the protein [10]. Thus, based on a statistical analysis of about 50 globular proteins, the total change in surface area ΔASA can be written:

$$\Delta ASA\left(\text{Å}^2\right) = -907 + 93 \times n_{aa}. \quad (1)$$

ΔASA and ΔC_p are linked by the following relationship [10]:

$$\Delta C_p\left(\text{cal mol}^{-1}\ \text{K}^{-1}\right) = -119 + 0.20 \times \Delta ASA\left(\text{Å}^2/\text{molecule}\right). \quad (2)$$

Eq. (2) is a very useful empirical rule to predict ΔC_p accompanying unfolding of monomeric globular proteins and reveals an underlying similarity in the degree of folding which is independent of the primary sequence. In other words, different monomeric globular protein folds are based on the same kinds of interactions. Folding of proteins to their native state is generally driven by hydrophobic interactions, where the non-polar side groups tend to be buried in the interior of the protein while the polar side groups will tend to remain exposed. In

* Corresponding author. Center for Insoluble Protein Structures (inSPIN), Interdisciplinary Nanoscience Centre, University of Aarhus, Gustav Wieds Vej 10C, DK-8000 Aarhus C, Denmark. Tel.: +45 89 42 50 46; fax: +45 86 12 31 78.
E-mail address: dao@inano.dk (D.E. Otzen).

0301-4622/$ – see front matter © 2010 Elsevier B.V. All rights reserved.
doi:10.1016/j.bpc.2010.03.016

contrast, fibril formation is driven by strong backbone interactions which may lead to the unfavorable burial of polar and charged groups, leading to a decrease in the ΔC_p [12,13]. Due to the complexity and the many steps involved in the fibrillation mechanism, fibril formation may be under kinetic control, so that the end structure is not necessarily the one with the lowest possible energy [14]. Furthermore, the fibrils are organized in quaternary structures which can lead to a larger ΔASA compared to native folded protein, though this may be counterbalanced by the surface exposure of parts of the protein which are not incorporated into the fibrillar structure and may remain at least partially unfolded. The quaternary structures also open for the possibility of water being buried in the fibril interior, leading to a positive or negative ΔC_p, depending on whether the water interacts with hydrophobic or hydrophilic residues [15]. The extensive hydrogen bond network together with the dipole–dipole interaction of the peptide backbone, will also contribute to the heat capacity [16,17]. It has been showed that fibrils reorganize under pressure, suggesting that they are not packed optimally [16]. Another factor that may contribute significantly to ΔC_p is the creation or change in solvation of electrostatic charges [18]. Molecular dynamics simulations suggest that β-sheets may associate through a dehydration of the hydrogen bonding groups by "wrapping" them in neighboring hydrophobic side chains [17]. The removal of screening water will strengthen the hydrogen bond and can make this the dominant factor driving β-sheet association. Folding-associated changes in intramolecular vibrations (which have energies on the same level as thermal energy) have also been estimated to contribute to ΔC_p [18]. As the fibrils are built on a large degree of inter-molecular hydrogen bonding, the degrees of freedom will decrease compare to the native state, though the less optimal side chain packing in the fibrils will give rise to more intra-molecular vibrations.

All these factors contribute to the ΔC_p of fibrillation, but in ways that are difficult to predict. Very few studies have focused on the relationship between fibrillar structure and thermodynamic properties. The pioneering work by Kardos, Goto and coworkers revealed that the ΔC_p accompanying formation of native and fibrillated β_2-microglobulin from the unfolded peptide are very similar [19]. Clearly more data on, and further insights into, the ΔC_p associated with fibrillation are needed, with the ultimate goal of better understanding the structure and formation of fibrils.

That aim may be promoted by exploiting the phenomenon of fibrillar polymorphism, where the same peptide can give rise to completely different structures. Using the 29-residue peptide hormone glucagon as a model system for aggregation, we have shown that changes in environment factors such as pH, temperature, peptide concentration, salt and pressure can profoundly change the structure of the end-point fibrils [14,20–24]. Polymorphism is expected to affect the ΔC_p due to differences in compactness, side change interactions and water content. Fibrillation at different pH values will also incur different enthalpies of ionization associated with the uptake and release of protons [25].

Here we modulate glucagon fibrillar structure with buffers and salts to investigate the coupling between fibril structure and thermodynamic properties. We find the change in heat capacity upon fibrillation to be highly dependent on the environment. The measured ΔC_p values exceed the values expected from data on globular proteins. NaCl type fibrils are less stable than the other fibrils and have a large and positive ΔC_p, which may reflect underlying changes in the fibrillar structure.

2. Materials and methods

2.1. Materials

Pharmaceutical grade glucagon (HSQGTFTSDYSKYLDSRRAQDFVQWLMNT) was purified (>98.9%) by Novo Nordisk A/S (Gentofte, Denmark). Thioflavin T was obtained from Sigma-Aldrich (St. Louis, Ohio, USA) and used without further purification. All other chemicals were from Sigma or Fluka.

2.2. Generation of glucagon fibrils

Glucagon powder was dissolved in a single step to a concentration of 0.5 mg/ml in three different buffers, namely (1) 50 mM glycine pH 2.5, (2) 5 mM HCl with 150 mM NaCl and (3) 10 mM HCl with 1 mM Na_2SO_4. The ensuing fibrils are referred to as glycine, NaCl and sulfate fibrils, respectively. The solution was fibrillated by incubating it for 24 h at 37 °C with vigorous shaking. For subsequent analysis, the samples were centrifuged for 10 min before aspiration of the supernatant. The pellet was washed in milliQ water and centrifuged again before resuspension in milliQ water to a concentration of 0.5 mg/ml glucagon. The fibrils were sonicated for 30 s with a sonicator energy of 70% (BANDELIN Electronic GmbH, Berlin, Germany).

2.3. Solid state circular dichroism

The spectra were recorded at the SRCD facility at the UV1 beamline [26] on the storage ring ASTRID at Institute for Storage Ring Facilities (ISA), University of Aarhus, Denmark as previously described [27]. An MgF_2 plate was thoroughly cleaned with milliQ water and dried before a baseline spectrum was collected. A 20-μl sample was then applied as a droplet of approximately ellipsoid shape. The sample was dried for 10 min and the spectra were recorded over a wavelength range of 330–130 nm in 1 nm steps. After cleaning the plate, a second baseline spectrum was recorded.

2.4. X-ray fiber diffraction analysis

Fiber diffraction samples were prepared on a stretch frame using a starting suspension of approximately 0.5 mg/ml aggregated glucagon, and dried at 30 °C. Data were collected in-house using a Cu Kα rotating-anode source (FR591 Enraf Nonius, Delft, Holland; wavelength 1.5418 Å), equipped with a MARResearch 345 image plate X-ray detector (345 mm diameter). The sample to detector distance was 425.8 mm with exposure times of 20–60 min. The images were evaluated using CLEARER (http://www.lifesci.sussex.ac.uk/home/Louise_Serpell/).

2.5. Isothermal Titration Calorimetry (ITC)

The elongation of the glucagon fibrils was monitored using a VP isothermal titration calorimeter from MicroCal (Northampton, USA). 1 mg/ml glucagon was titrated into 1.4 ml of 0.5 mg/ml glucagon fibrils in 50 mM glycine–HCl buffer (pH 2.5) at 25 °C. The solutions were degassed under vacuum with a ThermoVac accessory from MicroCal. An initial injection of 3 μl was followed by 1 injection of 40 μl. The 40 μl peak area was integrated using ITC Data Analysis in MicroCal Origin 7.0.

2.6. Acrylamide quenching

Quenching studies were performed in a 96-well microtiter plate. 0.5 g/l glucagon was added to all the wells and diluted 1:1 with an acrylamide solution to give a final acrylamide concentration of 0–750 mM. The emission intensity was measured at 330 nm and 354 nm using excitation at 295 nm.

2.7. Proteolysis experiments

Proteolysis experiments were carried out by incubating 0.5 mg/ml glucagon fibrils with elastase. Enzymatic digestions were all performed in 50 mM HEPES buffer (pH 7) at 37 °C using enzyme:

substrate ratios of 1:10 and 1:100 (w/w). The persistence of intact glucagon at different time points during proteolysis was monitored by SDS-PAGE using a Tricine Gel which was subsequently stained with Coomassie Brilliant Blue for 12 h.

3. Results

To explore the link between the structural and thermodynamic properties of glucagon fibrils, we exploited glucagon's ability to form different fibrils under different conditions, namely (1) 150 mM NaCl and 5 mM HCl (referred to as salt fibrils); (2) 1 mM Na_2SO_4 and 10 mM HCl (sulfate fibrils) and (3) 50 mM glycine pH 2.5 (glycine fibrils). We analyzed the 3 types of fibrils using a combination of structural (synchrotron radiation CD, fiber diffraction), thermodynamic (ITC), spectroscopic (acrylamide quenching) and dynamic (proteolysis) assays.

3.1. Thermodynamic data

To obtain information about the change in heat capacity (ΔC_p) upon fibrillation, we titrate monomeric glucagon into an ITC cell with a solution of glucagon fibrils (Fig. 1A) to obtain the enthalpy of elongation ΔH_{obs} at different temperatures [19]. We conclude that all the glucagon monomers are taken up into fibrils since repeated measurements of the elongation step at a given temperature provide the same elongation data, with no indication of saturation (data not shown). Furthermore, independent experiments under similar conditions show that >95% of all glucagon can be spun down as a pellet after the completion of fibrillation (data not shown). This implies that the reaction goes to completion under all conditions, though nothing can directly be inferred about the free energy associated with the reaction since the fibrillation process is essentially irreversible.

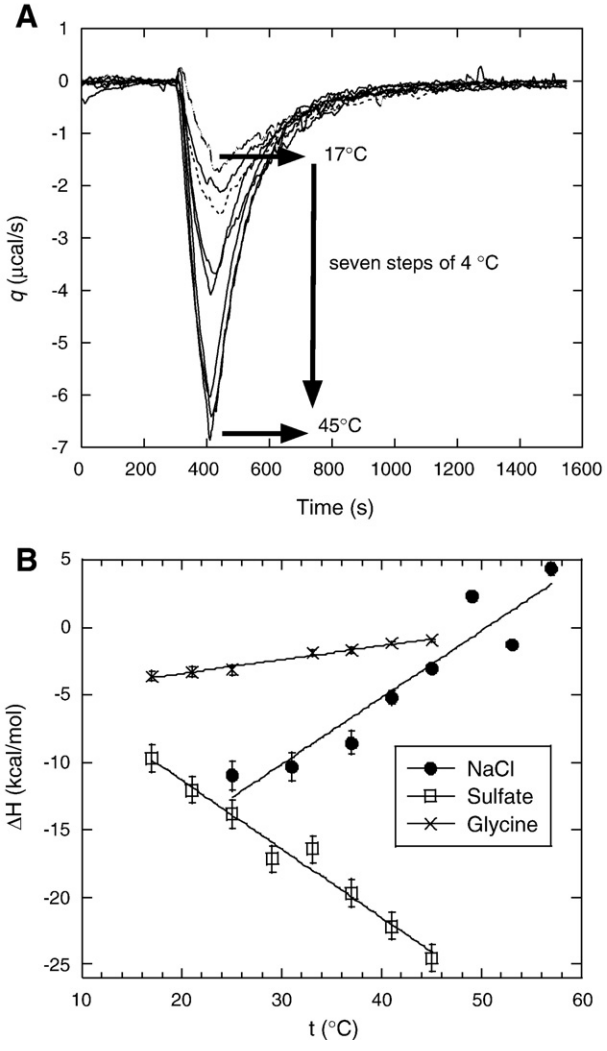

Fig. 1. Measured heat capacity changes ΔC_p associated with glucagon fibrillation are highly dependent on buffer conditions. (A) Temperature dependence of the elongation enthalpy ΔH_{obs} in sulfate buffer (10 mM HCl + 1 mM Na_2SO_4). Cell: 0.5 g/l fibrils. Syringe: 40 µl 1 g/l glucagon monomers injected after 300 s. (B) ΔC_p determined as the temperature dependence of ΔH_{obs} measured in the three different buffer conditions (150 mM NaCl 5 mM HCl, 1 mM Sulfate 50 mM glycine buffer pH 2.5, 50 mM glycine buffer pH 2.5 respectively). Error bars based on triplicate measurements.

The ITC elongation experiments were carried out over a temperature interval spanning 17–57 °C, and the elongation enthalpy was in each case obtained as an average of five monomer injections. By plotting ΔH_{obs} versus temperature, we obtain ΔC_p as the slope of the linear fit (Fig. 1B). ΔC_p values for the three fibril types are summarized in Table 1 and show a large variation among the three different fibril types. Both glycine and salt fibrils show positive ΔC_p values, while that of the sulfate fibrils is large and negative.

At this stage it is important to note that the release or uptake of protons accompanying the fibrillation process may make significant contributions to the measured enthalpy and thus the measured ΔC_p of fibrillation [25,28–30]. This can be directly quantified. Fibrillation studies of glucagon in buffers with different ionization enthalpies reveal that ~5 protons are released every time a glucagon molecule is incorporated into a fibril in glycine buffer [25]. The elongation of a fibril can be schematically represented as one monomer (M) attaching to a pre-existing fibril containing m monomers (F_m), leading to the exchange of n protons:

$$M - n\mathrm{H}^+ + F_m + buffer \leftrightarrow F_{m+1} + buffer - n\mathrm{H}^+ \quad (3)$$

The observed enthalpy for fibril elongation (ΔH_{obs}) may be expressed as [31,32]:

$$\Delta H_{obs} = \Delta H_{intrinsic} + \Delta H_{ion} \times n_{H+} \quad (4)$$

where ΔH_{ion} is the ionization enthalpy of the buffer and $\Delta H_{intrinsic}$ is the fibrillation enthalpy change in the absence of buffer contributions. Likewise the measured ΔC_p^{obs} can be expressed as:

$$\Delta C_p^{obs} = \Delta C_p^{intrinsic} + \Delta C_p^{ion} \times n_{H+} \quad (5)$$

where ΔC_p^{ion} is the change in ionization heat capacity of the buffer and $\Delta C_p^{intrinsic}$ is the fibrillation heat capacity change in the absence of buffer contributions. As seen in Fig. 2, ΔC_p^{ion} for the glycine buffer is 0.02 kcal/K/mol. Given that 5 protons are exchanged [25], this gives a

Table 1
Summary of structural and thermodynamic properties of the three different fibril types.

	Glycine	Sulfate	NaCl
k_{SV}^{Fibril} (M^{-1}) [a]	1.49	2.75	2.36
$k_{SV}^{Monomer}$ (M^{-1}) [a]	15.27	15.36	15.45
$\Delta C_p^{intrinsic}$ (kcal/mol/K) [b]	~0.02 ± 0.01	−0.51 ± 0.05	0.49 ± 0.07
ΔC_p^{buffer} (kcal/mol/K) [b]	0.0208 ± 0.0002	0.00 ± 0.00	0.00 ± 0.00
CD peak (nm)	224	227	222
CD peak (nm)	201	210	196
CD peak (nm)	176	191	179
CD peak (nm)	159	179	152
CD peak (nm)	148	156	
Fiber diffraction peaks (Å)	4.80	4.76	4.88
	6.07	5.7	5.3
	9.2	10.6	6.5
	10	13.1	16.2
	20	32	
	30		

[a] From acrylamide quenching studies.
[b] From ITC titration measurements.

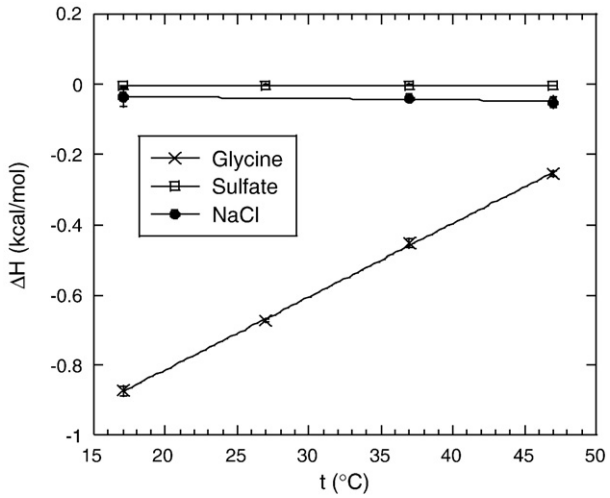

Fig. 2. Buffer protonation enthalpy as a function of temperature measured by ITC. The protonation enthalpy was obtained by injecting 5 times 5 μl HCl into the buffer. Buffer compositions as in legend to Fig. 1. The error bars are based on 5 injections.

total ΔC_p^{ion} of 0.1 kcal/K/mol, which corresponds remarkably well to the measured value of $\Delta C_p^{obs} = 0.12$. It can hereby be concluded that ΔC_p for the fibrillation of glucagon in glycine buffer $\Delta C_p^{intrinsic} \sim 0$.

In contrast to the glycine buffer, no buffer ionization occurs in HCl/NaCl and HCl/Na_2SO_4 (Fig. 2). This means that the measured ΔC_p values correspond to $\Delta C_p^{intrinsic}$.

As discussed in the Introduction, unfolding increases the protein's heat capacity primarily due to additional hydration of hydrophobic residues. Protein aggregation such as fibrillation would be expected to lead to negative ΔC_p since it normally buries surface area [19]. These observations suggest that the simple relationships between changes in surface area and ΔC_p derived for the folding/unfolding process cannot in general be used to rationalize heat capacity changes following fibrillation.

The interpretation of the slopes in Fig. 1B as ΔC_p assumes that the structure of the "reactants" and "products" in the fibrillation process is independent of the temperature over the interval studied here. In other words, the structural transformation that a monomer undergoes upon association with the existing fibril should be similar at all temperatures. To verify this, we conducted the following experiments.

Firstly, we probed the compactness of the distinct glucagon fibrils as a function of elongation temperature by a simple quenching experiment, in which the tryptophan fluorescence F_o is quenched to the value F by increasing concentrations of the neutral quencher acrylamide (Q). The efficiency by which this occurs is determined by a plot of F_o/F versus acrylamide concentration, in which the slope provides the Stern Volmer constant k_{SV}. k_{SV} provides information about the tryptophan accessibility and thus indirectly fibril compactness [33]. k_{SV} was obtained from 4 samples made under different temperatures (Fig. 3 and Table 1). Over the temperature range 23–43 °C, k_{SV} is essentially constant, and is significantly lower (~1.5 M^{-1}) for glycine fibrils than for the salt and sulfate fibrils (~2.4 and 2.8 M^{-1}, respectively). This indicates that the tryptophan is significantly more exposed in the salt and sulfate fibrils than in the glycine fibrils, although the values are in all cases much lower than k_{SV} ~15 M^{-1} measured for monomeric glucagon in all 3 buffers (Table 1).

Secondly, we probed the structure of the monomeric glucagon by circular dichroism after an incubation time of 2 h (mimicking conditions for the ITC experiment where the monomer solution is incubated in the syringe for up to 2 h before injection). We observe no significant difference in the structure of the monomer as a function of incubation temperature (data not shown).

Thus, the current structural investigations do not identify any changes in compactness.

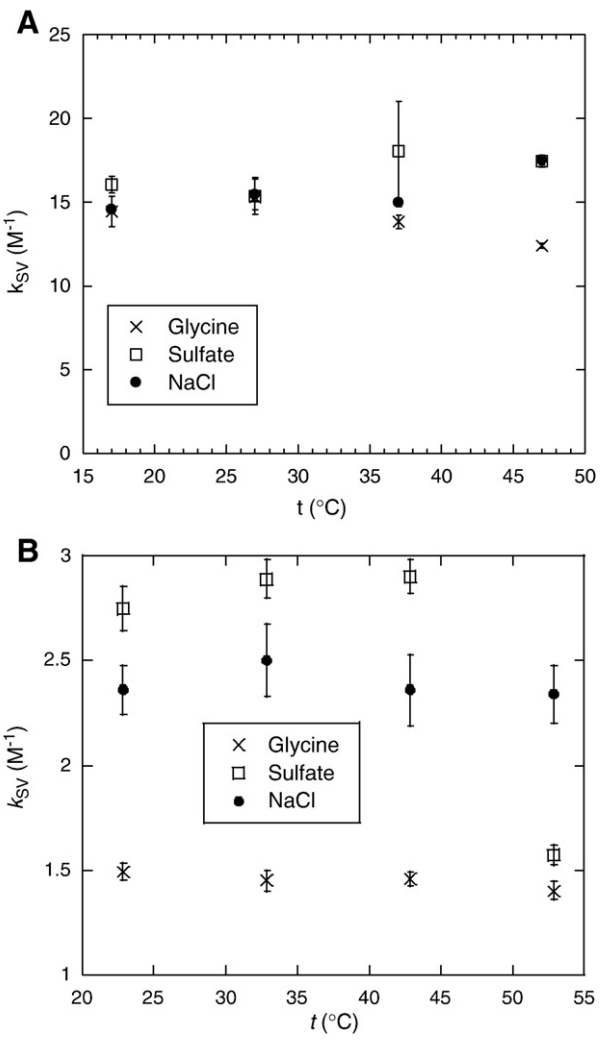

Fig. 3. Stern Volmer constants k_{SV} as function of temperature for the three fibril types. The intrinsic Trp fluorescence of the 3 different fibril types was quenched by the addition of acrylamide to (A) monomeric and (B) fibrillated glucagon. The emission intensity was measured at 330 nm and 354 nm using excitation at 295 nm. The error bars are based on triplicate measurements.

3.2. Elastase proteolysis experiments confirm that the fibrils made in glycine buffer are the most compact fibrils

To analyze the compactness and structural dynamics of the different glucagon fibrils, we investigated their resistances towards proteolytic digestion by SDS-PAGE (Fig. 4). Clearly the glycine fibrils are the least susceptible to degradation, while both salt and sulfate fibrils are essentially completely degraded at glucagon:protease molar ratios of 1:10. This ranking agrees nicely with the quenching data to establish that the glycine fibrils are the most compact and the salt and sulfate fibrils equally exposed.

3.3. Fiber diffraction show large difference between the three types of glucagon fibrils

X-ray fibre diffraction is a well established technique to measure repetitive molecular spacings in fibrils [34]. Typically the most prevalent distance is the β-strand spacing around 4.8 Å and the β-sheet spacing around 10–12 Å.

Fiber diffraction patterns of the three glucagon fibril types confirmed underlying differences in structures (Fig. 5). The characteristic β-strand distance varied from 4.76 to 4.88 Å and the fibrils differed substantially in other peaks. For the glycine type fibril, we

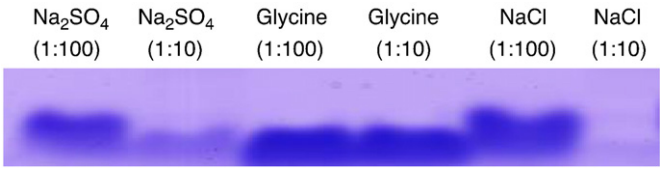

Fig. 4. Proteolytic sensitivity of the three different glucagon fibrils. Fibrils were spun down and the supernatant was removed. The fibrils were resuspended in 50 mM HEPES buffer (pH 7) and incubated with elastase at protease:substrate ratios of 1:10 and 1:100 (w/w) at 37 °C for 4 h. The figure shows the bands of molecular weight corresponding to full-length glucagon (3 kDa).

observe a classical fibril pattern with distances of 4.8 Å and 10.0 Å. Furthermore we also observe distances of 20 Å and 30 Å which probably correspond to double and triple inter-sheet distances, indicating a fibril of a least four layers. The sulfate type fibrils show significant differences compared to the glycine fibrils, with peaks at 4.76 Å and 10.6 Å (Fig. 5), but lack the peaks at 20 Å and 30 Å, indicating that the sulfate fibrils consist of only a double layer. The NaCl type fibril is distinguished by strong peaks at 6.36 Å, 5.32 Å, 4.88 Å and only a very weak peak around 15 Å, which suggests a very different structural arrangement.

3.4. Synchrotron radiation circular dichroism spectra of glucagon fibrils reveal underlying changes

To obtain information about how related the three types of glucagon fibrils are compared to fibrils made from other proteins, we recorded synchrotron radiation circular dichroism spectra for the three types of glucagon fibrils. The CD spectra of the three types of dried glucagon fibrils differ very much from each other (Fig. 6). The CD spectrum for the sulfate fibrils has features resembling α-helices with minima around 226 and 209 nm and a peak at 191 nm. Both salt and glycine fibrils show a more conventional β-sheet spectrum [35] with a single deep minimum around 222–224 nm and peaks around 196–204 nm. Nevertheless, the two fibrils differ in the absolute intensity of the signals as well as the distribution of shoulder and peak in the absorption around 196–204 nm.

4. Discussion

In this study we have performed a thermodynamic analysis of three glucagon fibril types formed under different buffer conditions. The structural differences of the three different glucagon fibril morphologies have been well described in previous studies [14,22] and are substantiated and extended by our present observations. We observe a remarkable variation in ΔC_p values for the three types of fibrils, ranging from strongly negative (sulfate fibrils) over zero (glycine fibrils) to strongly positive (salt fibrils). The positive ΔC_p values do not arise from increased exposure of fibrils at higher elongation temperature or increased compaction of the monomer, as our acrylamide quenching experiments indicate no significant change in exposure in the measured temperature interval.

In the following section, we discuss various factors which may contribute to the ΔC_p of the glucagon fibrils.

4.1. Burial of hydrophobic surface area

The ΔC_p values for glucagon fibrillation are in stark contrast to the well established theories of predicting ΔC_p from the ΔASA through ΔASA's linear correlation to the size of the protein. Using Eq. (2) [10], the 29-residue glucagon is predicted to have a ΔC_p of −0.24 kcal/mol/K. This is only about 50% of what we see for the sulfate type glucagon fibrils, and obviously very different from the other ΔC_p values. Both acrylamide quenching and proteolysis experiments indicate that the glycine fibrils are the most compact fibril species while the sulfate and salt fibrils appear equally exposed. Based on this, we would predict that the glycine fibrils should show the largest negative ΔC_p value and the sulfate and salt fibrils should show smaller but still negative values. The obvious discrepancy with the measured ΔC_p values shows that compactness (and by inference ΔASA) is not a useful predictor of fibrillar ΔC_p.

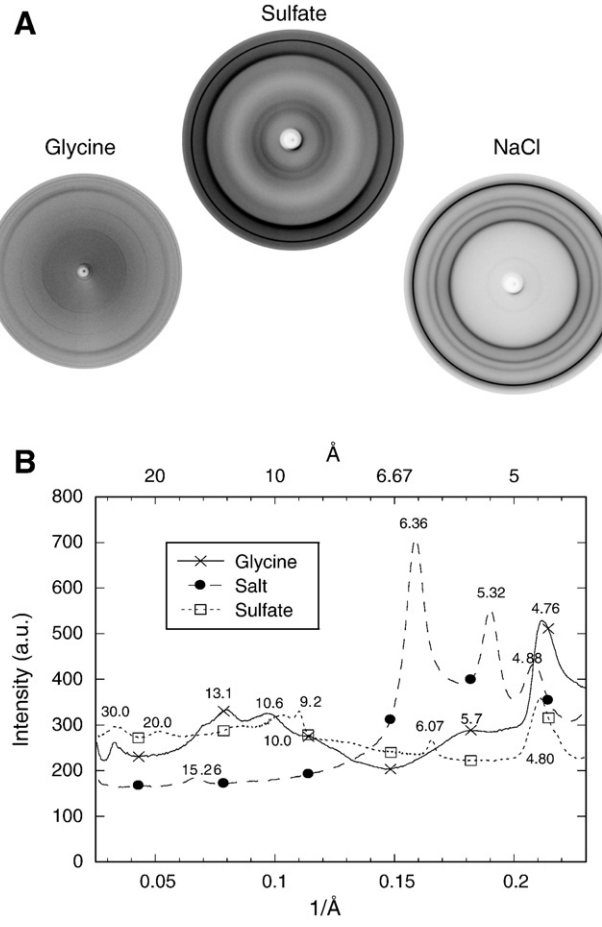

Fig. 5. Fiber diffraction of glucagon fibrils. (A) Diffraction patterns of the three different glucagon fibrils. (B) Intensities derived from the diffraction pattern shown in panel A.

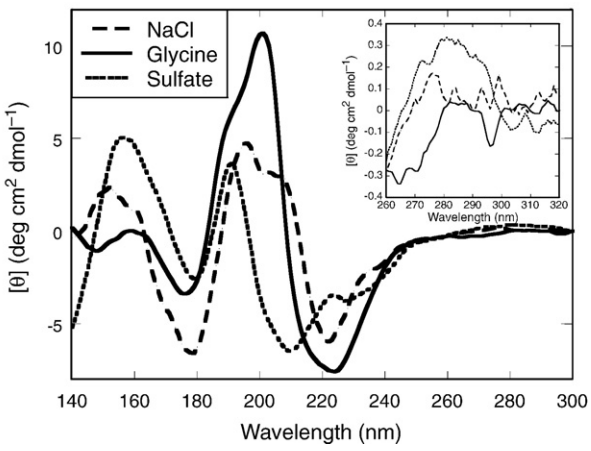

Fig. 6. Solid state circular dichroism spectra for the three types of glucagon fibrils. The inset shows a zoom in the aromatic region of the UV spectrum.

4.2. Incorporation of ions into the structure

Electrostatic interactions can also contribute to ΔC_p, since the breaking of a salt bridge can increase ΔC_p by 20–50 cal/K/mol [18]. Nevertheless, even if, as an extreme scenario, we assume that each glucagon monomer (which has 5 positive charges at low pH) can bind 5 anions which are all displaced upon forming the fibrils, we can only expect a positive contribution of 0.1–0.25 kcal/mol/K, which is well below the 0.5 kcal/mol/K measured for salt fibrils and obviously far from the negative values observed for sulfate fibrils.

4.3. Buried water molecules

Buried water can have a stabilizing effect on the protein structure. Water inside the interior will increase the hydrogen bonding potential and provide better van der Waals interactions than an empty cavity [36], but there will be an entropic penalty as well as a penalty for hydration of non-polar groups [37]. In practice, this leads to a negative ΔC_p when the water molecule is close to a hydrophobic residue [15], but a positive ΔC_p when the water is coordinated by a polar or charged residue [38].

4.4. Burial of hydrophilic/charged residues

Hydrophilic and charged residues have a strong tendency to be solvated. For globular proteins, the polar groups will remain in contact with the water, leading to an insignificant ΔC_p contribution [18]. Conversely, amyloid formation may lead to unfavorable side chain interactions due to strong main chain interactions [3]. When a polar side chain is forced into a non-polar interior, ΔC_p will be positive [15]. It has been shown that substitution of a buried non-polar group by a polar group will increase the ΔC_p much more than what is predicted based on ΔASA [12]. Likewise it has been found that burial of charged and polar groups upon binding can give rise to a positive ΔC_p [39].

4.5. Salt dependent fibril morphologies lead to unique ΔC_p values

The fiber diffraction spectra are consistent with quenching and protease data in revealing that the glycine type fibril is the most compact, given that the inter-strand distances for the glycine; sulfate and salt fibrils are 4.7; 4.8 and 4.9 Å, respectively. We speculate that the $Na^+/Cl^-/SO_4^{2-}$ ions may bind to the inter-strand spaces and thus drive them further apart. Binding of ions may also lead to the salt fibrils' unique fiber diffraction peaks where the characteristic band around 10–11 Å from inter-sheet packing is missing. It has been suggested that bound inorganic ions could reduce the ability to form inter-sheet packing or lead to a mixture of both parallel and anti-parallel sheets which will strongly attenuate the 10–11 Å band [40,41]. In contrast to NaCl, even low millimolar concentrations of Na_2SO_4 stabilize the glucagon fibrils [14]. This strong effect must arise from direct electrostatic interactions between the positively charged groups and the SO_4^{2-} ions.

We have found that the heat capacity change associated with the fibrillation of glucagon depends strongly on the fibril structure. The observed per-residue changes in ΔC_p are numerically large compared to typical values for the folding of small globular proteins. These observations suggest that the hydration of the peptide varies markedly in different buffers. The key observation in this study is that there is no correlation between the compactness of the fibrils (as determined by acrylamide quenching, proteolysis experiments and fiber diffraction) and the change in heat capacity. The reason for the missing correlation between ΔASA and ΔC_p is probably the characteristic fibril architecture, which may lead to subtle changes in the contributions to ΔC_p outlined in the previous section. Strong backbone interactions may lead to the unfavorable burial of polar side residues, water and/or charged groups which all can have major influence on the change in ΔC_p. For the glucagon fibrils elongated in the presence of 150 mM NaCl, we observed a highly positive ΔC_p (0.49 ± 0.007 kcal/mol/K) upon fibrillation. One scenario, admittedly speculative, is that the high salt concentration promotes the fibrillation to such a degree that it becomes kinetically trapped in a conformation which is not the most stable in thermodynamic terms. The fibril may thus harbor unfavorable side change interactions and buried water molecules. If the salt fibrils represent a kinetic trap, this implies that they are formed because of a specific sequence of events rather than because of their innate stability. This would not be unexpected in view of the high kinetic barriers associated with protein aggregation in general. We have previously suggested that glucagon's high sensitivity to environmental conditions during fibrillation is likely to induce a "kinetic fitness selection" [42]. To demonstrate the kinetic stability of these salt fibrils, it would be necessary to show that fibrils prepared in a different manner (*e.g.* starting from another pH, increasing the salt concentration stepwise, etc.) but leading to the same final conditions (here 150 mM NaCl, pH 2) would have different properties. We are currently investigating this possibility.

The fact that the NaCl fibrils behaves differently is confirmed in the fiber diffraction pattern of the NaCl type fibrils which show a large divergence in the fibril structure compared to the other two types of glucagon fibrils.

For the sulfate type fibrils, we see a larger change in ΔC_p (-0.51 ± 0.05 kcal/mol/K) than expected based on Eq. (2) (-0.24 kcal/mol/K). We find this difficult to explain. We hesitate to attribute the large change in ΔC_p to fibrils' ability to form quaternary structures, resulting in a larger ΔASA compared to native folding, since this should also be the case for the other two fibrils.

Finally the relatively low change in ΔC_p (0.02 ± 0.01 kcal/mol/K) for the glycine fibril could be a result of unfavorable packing interactions which cancel out other contributions, though this will not occur to the same extent as we see it for the NaCl type fibrils.

It is to be hoped that atomic-level structural information may help us elucidate the structural basis for these intriguing differences, though it is possible that it may be difficult to pinpoint subtle changes in hydration and ion binding. Efforts to achieve this are currently underway.

In summary, we have shown that glucagon fibrils formed under three different conditions differ markedly in the heat capacity of their formation, and this variation cannot be explained on the basis of different degrees of compaction as determined by acrylamide quenching, proteolysis resistance or fiber diffraction data. Possible explanations include changes in solvation, ion binding and unfavorable side chain packing. High-resolution structures of these fibrils can potentially provide further insight into these remarkable phenomena.

Acknowledgements

M.D.J. and D.E.O. are supported by the Danish Research Science Foundation through inSPIN. We are grateful to Dr. Hans Aage Hjuler from Novo Nordisk A/S for generously providing glucagon and for many constructive discussions on glucagon fibrillation. We thank Dr. Anders Malmendal for useful discussions on glucagon fibrillation.

References

[1] F. Chiti, C.M. Dobson, Protein misfolding, functional amyloid, and human disease, Annu. Rev. Biochem. 75 (2006) 333–366.
[2] A.P. Pawar, K.F. Dubay, J. Zurdo, F. Chiti, M. Vendruscolo, C.M. Dobson, Prediction of "aggregation-prone" and "aggregation-susceptible" regions in proteins associated with neurodegenerative diseases, J. Mol. Biol. 350 (2005) 379–392.
[3] M. Fandrich, C.M. Dobson, The behaviour of polyamino acids reveals an inverse side chain effect in amyloid structure formation, Embo J. 21 (2002) 5682–5690.
[4] C.M. Dobson, Protein misfolding, evolution and disease, Trends Biochem. Sci. 24 (1999) 329–332.
[5] K.E. Marshall, L.C. Serpell, Structural integrity of beta-sheet assembly, Biochem. Soc. Trans. 37 (2009) 671–676.

[6] T.R. Jahn, S.E. Radford, The Yin and Yang of protein folding, Febs J. 272 (2005) 5962–5970.
[7] M. Vendruscolo, C.M. Dobson, Towards complete descriptions of the free-energy landscapes of proteins, Philos. Trans. A Math. Phys. Eng. Sci. 363 (2005) 433–450 discussion 450-432.
[8] S.N. Timasheff, Protein hydration, thermodynamic binding, and preferential hydration, Biochemistry 41 (2002) 13473–13482.
[9] K.P. Murphy, V. Bhakuni, D. Xie, E. Freire, Molecular basis of co-operativity in protein folding. III. Structural identification of cooperative folding units and folding intermediates, J. Mol. Biol. 227 (1992) 293–306.
[10] J.K. Myers, C.N. Pace, J.M. Scholtz, Denaturant m values and heat capacity changes: relation to changes in accessible surface areas of protein unfolding, Protein Sci. 4 (1995) 2138–2148.
[11] R.S. Spolar, J.R. Livingstone, M.T. Record Jr., Use of liquid hydrocarbon and amide transfer data to estimate contributions to thermodynamic functions of protein folding from the removal of nonpolar and polar surface from water, Biochemistry 31 (1992) 3947–3955.
[12] V.V. Loladze, D.N. Ermolenko, G.I. Makhatadze, Heat capacity changes upon burial of polar and nonpolar groups in proteins, Protein Sci. 10 (2001) 1343–1352.
[13] S. Xu, Cross-beta-sheet structure in amyloid fiber formation, J. Phys. Chem. B 113 (2009) 12447–12455.
[14] J.S. Pedersen, J.M. Flink, D. Dikov, D.E. Otzen, Sulfates dramatically stabilize a salt-dependent type of glucagon fibrils, Biophys. J. 90 (2006) 4181–4194.
[15] K. Kano, Y. Ishida, K. Kitagawa, M. Yasuda, M. Watanabe, Heat-capacity changes in host–guest complexation by Coulomb interactions in aqueous solution, Chem. Asian J. 2 (2007) 1305–1313.
[16] E. Chatani, Y. Goto, Structural stability of amyloid fibrils of beta(2)-microglobulin in comparison with its native fold, Biochim. Biophys. Acta 1753 (2005) 64–75.
[17] A. Fernandez, What factor drives the fibrillogenic association of beta-sheets? FEBS Lett. 579 (2005) 6635–6640.
[18] J.M. Sturtevant, Heat capacity and entropy changes in processes involving proteins, Proc. Natl Acad. Sci. USA 74 (1977) 2236–2240.
[19] J. Kardos, K. Yamamoto, K. Hasegawa, H. Naiki, Y. Goto, Direct measurement of the thermodynamic parameters of amyloid formation by isothermal titration calorimetry, J. Biol. Chem. 279 (2004) 55308–55314.
[20] C.B. Andersen, D. Otzen, G. Christiansen, C. Rischel, Glucagon amyloid-like fibril morphology is selected via morphology-dependent growth inhibition, Biochemistry 46 (2007) 7314–7324.
[21] M.S. Celej, W. Caarls, A.P. Demchenko, T.M. Jovin, A triple emission fluorescent probe reveals distinctive amyloid fibrillar polymorphism of wild-type alpha-synuclein and its familial Parkinsons disease mutants, Biochemistry 48 (2009) 7465–7472.
[22] J.S. Pedersen, D. Dikov, J.L. Flink, H.A. Hjuler, G. Christiansen, D.E. Otzen, The changing face of glucagon fibrillation: structural polymorphism and conformational imprinting, J. Mol. Biol. 355 (2006) 501–523.
[23] J.S. Pedersen, D.E. Otzen, Amyloid—a state in many guises: survival of the fittest fibril fold, Protein Sci. 17 (2008) 2–10.
[24] S.J. Wood, B. Maleeff, T. Hart, R. Wetzel, Physical, morphological and functional differences between ph 5.8 and 7.4 aggregates of the Alzheimer's amyloid peptide Abeta, J. Mol. Biol. 256 (1996) 870–877.
[25] M. Jeppesen, P. Westh, D.E. Otzen, The role of protonation in protein fibrillation, FEBS Lett. 584 (2010) 780–784.
[26] S. Eden, P. Limão-Vieira, S.V. Hoffmann, N.J. Mason, VUV photoabsorption in CF3X (X = Cl, Br, I) fluoro-alkanes, Chem. Phys. 323 (2005) 313–333.
[27] L.W. Nesgaard, S.V. Hoffmann, C.B. Andersen, A. Malmendal, D.E. Otzen, Characterization of dry globular proteins and protein fibrils by synchrotron radiation vacuum UV circular dichroism, Biopolymers 89 (2008) 779–795.
[28] B.M. Baker, K.P. Murphy, Evaluation of linked protonation effects in protein binding reactions using isothermal titration calorimetry, Biophys. J. 71 (1996) 2049–2055.
[29] C.M. Barbieri, D.S. Pilch, Complete thermodynamic characterization of the multiple protonation equilibria of the aminoglycoside antibiotic paromomycin: a calorimetric and natural abundance ^{15}N NMR study, Biophys. J. 90 (2006) 1338–1349.
[30] A.G. Kozlov, T.M. Lohman, Large contributions of coupled protonation equilibria to the observed enthalpy and heat capacity changes for ssDNA binding to *Escherichia coli* SSB protein, Proteins Suppl. 4 (2000) 8–22.
[31] H. Fukada, H. Takahashi, Enthalpy and heat capacity changes for the proton dissociation of various buffer components in 0.1 M potassium chloride, Prot. Struct. Funct. Genet. 33 (1998) 159–166.
[32] B.M. Baker, K.P. Murphy, Evaluation of linked protonation effects in protein binding reactions using isothermal titration calorimetry, Biophys. J. 71 (1996) 2049–2055.
[33] M.R. Eftink, C.A. Ghiron, Exposure of tryptophanyl residues in proteins. Quantitative determination by fluorescence quenching studies, Biochemistry 15 (1976) 672–680.
[34] M. Sunde, L.C. Serpell, M. Bartlam, P.E. Fraser, M.B. Pepys, C.C. Blake, Common core structure of amyloid fibrils by synchrotron X-ray diffraction, J. Mol. Biol. 273 (1997) 729–739.
[35] S.Y. Venyaminov, J.T. Yang, in: G.D. Fasman (Ed.), Circular Dichroism and the Conformational Analysis of Biomolecules, Plenum Press, New York, 1996, pp. 69–107.
[36] R.C. Wade, M.H. Mazor, J.A. McCammon, F.A. Quiocho, A molecular dynamics study of thermodynamic and structural aspects of the hydration of cavities in proteins, Biopolymers 31 (1991) 919–931.
[37] K. Takano, Y. Yamagata, K. Yutani, Buried water molecules contribute to the conformational stability of a protein, Protein Eng. 16 (2003) 5–9.
[38] E.R. Guinto, E. Di Cera, Large heat capacity change in a protein-monovalent cation interaction, Biochemistry 35 (1996) 8800–8804.
[39] A. Niedzwiecka, J. Stepinski, E. Darzynkiewicz, N. Sonenberg, R. Stolarski, Positive heat capacity change upon specific binding of translation initiation factor eIF4E to mRNA 5' cap, Biochemistry 41 (2002) 12140–12148.
[40] O.S. Makin, P. Sikorski, L.C. Serpell, Diffraction to study protein and peptide assemblies, Curr. Opin. Chem. Biol. 10 (2006) 417–422.
[41] O. Sumner Makin, L.C. Serpell, Structural characterisation of islet amyloid polypeptide fibrils, J. Mol. Biol. 335 (2004) 1279–1288.
[42] J.S. Pedersen, D.E. Otzen, Amyloid — a state in many guises: survival of the fittest fibril fold, Protein Sci. 17 (2008) 1–9.